Received: 7 October 2022 | Accepted: 14 November 2022

DOI: 10.1002/pamm.202200122

Eigenvalue Optimization with respect to Shape-Variations in Electromagnetic Cavities

Christine Herter[1,*], **Sebastian Schöps**[2,**], and **Winnifried Wollner**[1,***]

[1] Universität Hamburg, Fachbereich Mathematik, Bundesstr. 55, 20146 Hamburg

[2] Computational Electromagnetics Group, Technische Universität Darmstadt, Schloßgartenstr. 8 64289 Darmstadt

The article considers the optimization of eigenvalues in electromagnetic cavities by means of shape variations. The field distribution and its frequency in a radio-frequency cavity are governed by Maxwell's eigenvalue problem. To this end, we utilize a mixed formulation by Kikuchi (1987) and a mixed finite element discretization by means of Nédélec and Lagrange elements. The shape optimization is based on the method of mappings, where a Piola transformation is utilized to assert conformity of the mapped spaces. We derive the derivatives by the use of adjoint calculus for the constraining Maxwell eigenvalue problem. In two numerical examples, we demonstrate the functionality of this method.

1 Introduction

Simulations of particle accelerator components are challenging due to high accuracy requirements. One important component is the superconducting radio-frequency cavity which is responsible for the acceleration of the particles. Cavities excite electromagnetic fields of various frequencies and for each frequency the corresponding electric field, so-called eigenmode, varies in its shape. The goal of a superconducting cavity is to achieve an acceleration mode to accelerate the particles forward. The most relevant acceleration eigenmode is the fundamental Transverse Magnetic (TM) mode, shown in Figure 1. For a detailed description of such a cavity as well as its associated components, we refer to the paper about Superconducting TESLA cavities by Aune et al. [2].

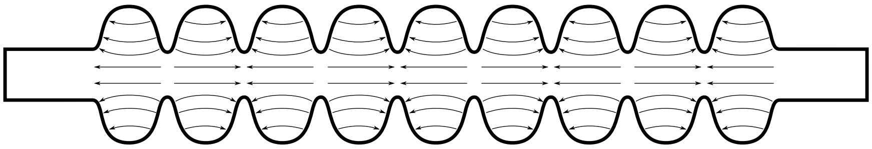

Fig. 1: Electric field of the TM_{010}, also called π-mode

The field distribution and its frequency are governed by Maxwell's eigenvalue problem

$$
\begin{aligned}
\nabla \times (\nabla \times u) &= \lambda u && \text{in } \Omega,\\
\nabla \cdot u &= 0 && \text{in } \Omega,\\
n \times u &= 0 && \text{on } \partial\Omega,\\
\|u\|^2 &= 1.
\end{aligned}
$$

In this work, we introduce a mixed variational formulation of Maxwell's eigenvalue problem by Kikuchi [8], which excludes the arising of so-called spurious modes (see also, e.g., Boffi [3]). The shape optimization is based on the method of mappings, where the physical domain Ω_q is given by a deformation $q\colon \widehat{\Omega} \to \mathbb{R}^d, d \in \{2,3\}$, on a reference domain $\widehat{\Omega} \subset \mathbb{R}^d$. To obtain suitable function spaces and equations on the reference domain suitable transformation rules need to be obeyed, e.g., for the function space $H_0(\text{curl};\widehat{\Omega})$ a Piola transformation is utilized to assert the conformity of the mapped spaces. The properties of the function spaces and corresponding mappings in detail are well explained by Monk [9]. For the resulting mixed variational formulation, we consider a computational domain given by a discretization of the space by using a mixed finite element method with Lagrange and Nédélec elements. The latter guarantees a correct subspace of $H_0(\text{curl};\Omega)$, see e.g. Monk [9]. We derive the derivatives by using adjoint calculus for the constraining Maxwell eigenvalue problem. The idea of using adjoint calculus to derive eigenvalue derivatives bases on Heuveline and Rannacher [7] and Rannacher, Westenberger and Wollner [10], where this approach is developed for elliptic eigenvalue problems. This article applies this approach to Maxwell's eigenvalue problem to achieve a free-form optimization for electromagnetic cavities.

* Corresponding author: e-mail christine.herter@uni-hamburg.de

** e-mail sebastian.schoeps@tu-darmstadt.de

*** e-mail winnifried.wollner@uni-hamburg.de

2 Mapping

Since we consider two different function spaces, we must distinguish between them with respect to the mapping to assert conformity of the mapped spaces. For details we refer to Monk [9] and Cohen [4], wherein the function spaces $H_0^1(\Omega)$ and $H_0(\text{curl}; \Omega)$ are well-explained in detail. In the following, we consider $\Omega_q, \hat{\Omega}$ as two bounded domains in $\mathbb{R}^d$, with $d \in \{2, 3\}$, where $x, \hat{x}$ denote coordinates on Ω_q and $\hat{\Omega}$. The deformation $F_q(\hat{x})$ is a mapping from $\hat{\Omega}$ to Ω_q given by

$$x = F_q(\hat{x}) = q(\hat{x}) + \hat{x}.$$

In addition, it holds that

$$\mathrm{d}x = \det(DF_q)\mathrm{d}\hat{x},$$

where DF_q is the Jacobian matrix of the displacement F_q, see Monk [9].

A scalar function $\hat{p} \in H_0^1(\hat{\Omega})$ is then transformed to a scalar function $p \in H_0^1(\Omega_q)$ by

$$p \circ F_q = \hat{p}.$$

Then it holds for $p \in H_0^1(\hat{\Omega})$ and $\hat{p} \in H_0^1(\hat{\Omega})$ that

$$\text{grad}\, p = DF_q^{-T} \text{grad}\, \hat{p}. \tag{1}$$

Furthermore, to transform vector functions in $H_0(\text{curl};\Omega)$, we apply a $H_0(\text{curl}; \Omega)$-conforming mapping to ensure tangential continuity. Therefore, we suppose $\hat{u} \in H_0(\text{curl}; \hat{\Omega})$ and an to $\hat{u}$ associated function $u \in H_0(\text{curl}; \Omega_q)$. For transforming $\hat{u}$ to u we use the so called covariant Piola mapping

$$u \circ F_q = DF_q^{-T}\hat{u}.$$

Then for $u \in H_0(\text{curl}; \Omega_q)$ and $\hat{u} \in H_0(\text{curl}; \hat{\Omega})$, it holds that in the three-dimensional case

$$\text{curl}\, u \circ F_q = \frac{1}{\det(DF_q)} DF_q \,\text{curl}\, \hat{u}.$$

In the two-dimensional case it holds that

$$\text{curl}\, u = \frac{1}{\det(DF_q)}\, \text{curl}\, \hat{u}.$$

In addition to that, we ensure that the determinant of the deformation gradient $\det(DF_q)$, which describes the volume ratio, has to be strictly larger than zero to satisfy physical properties.

3 Shape Optimization Problem

We consider a simply connected Lipschitz domain $\hat{\Omega} \subset \mathbb{R}^d$ $(d = 2, 3)$ with a control $q \in Q^{ad}$, where Q^{ad} is a vector-valued H^1-space and restrict the deformation tensor to

$$\infty > \det(DF_q) > 0.$$

The associated physical domain $\Omega_q = F_q(\hat{\Omega})$ is given by the mapping described in Section 2. The shape optimization problem of Maxwell's eigenvalue problem is defined as the following: Find a particular eigenvalue $\lambda \in \mathbb{R}$ and corresponding eigenvector $0 \neq u \in H_0(\text{curl}; \Omega_q)$ as solution of the problem

$$\min_{(\lambda,u,q)} J(q, (\lambda, u)) := \frac{1}{2}|\lambda - \lambda_*|^2 + \frac{\alpha}{2}\left(\|q\|^2 + \|\nabla q\|^2\right) - \beta \ln(\det(DF_q))$$

$$\text{s.t.} \quad \begin{aligned} \nabla \times (\nabla \times u) &= \lambda u && \text{in } \Omega_q \\ \nabla \cdot u &= 0 && \text{in } \Omega_q \\ n \times u &= 0 && \text{on } \partial\Omega_q \\ \|u\|_{\Omega_q}^2 &= 1, \end{aligned}$$

where $\|\cdot\|$ is the usual L^2 norm on $\hat{\Omega}$ while an index Ω_q refers to the respective norm on Ω_q, n is the outer unit normal vector to the boundary $\partial\Omega_q$, $\lambda_* \in \mathbb{R}$ the reference eigenvalue and $\alpha, \beta \in \mathbb{R}$.

We consider the variational formulation of Maxwell's eigenvalue problem introduced by Kikuchi [8] (, also seen in [3]): Find $\lambda \in \mathbb{R}$ and $0 \neq u \in H_0(\text{curl};\Omega_q)$ such that, for some $\psi \in H_0^1(\Omega_q)$

$$\begin{aligned} (\text{curl}\, u, \text{curl}\, v)_{\Omega_q} + (\text{grad}\, \psi, v)_{\Omega_q} &= \lambda(u,v)_{\Omega_q} \quad && \forall\, v \in H_0(\text{curl};\Omega_q) \\ (u, \text{grad}\, \varphi)_{\Omega_q} &= 0 && \forall\, \varphi \in H_0^1(\Omega_q) \end{aligned} \tag{2}$$

with the function spaces

$$\begin{aligned} H_0(\text{curl};\Omega_q) &= \left\{ v \in (L^2(\Omega_q))^d : \text{curl}\, v \in (L^2(\Omega_q))^n;\ v \times n = 0 \text{ on } \partial\Omega_q \right\}, \\ H_0^1(\Omega_q) &= \{ v \in H^1(\Omega_q) : v = 0 \text{ on } \partial\Omega_q \}, \end{aligned}$$

where $n = 1$ for $d = 2$ and $n = 3$ for $d = 3$.

We remind tha reader that, in the two-dimensional case, the curl operator is defined as a scalar, namely,

$$\text{curl}\, v = \frac{\partial v_2}{\partial x_1} - \frac{\partial v_1}{\partial x_2}.$$

We consider problem (2) on the reference domain $\hat{\Omega}$ and use the mapping, introduced in the previous section, to transform equations, e.g., for $d = 3$ to

$$\begin{aligned} (\text{curl}\, u, \text{curl}\, v)_{\Omega_q} &= \left(\frac{1}{\det(DF_q)}\, DF_q\, \text{curl}\, \hat{u}, DF_q\, \text{curl}\, \hat{v} \right)_{\hat{\Omega}}, \\ (\text{grad}\, \psi, v)_{\Omega_q} &= \left(\det(DF_q)\, DF_q^{-T} \text{grad}\, \hat{\psi}, DF_q^{-T}\, \hat{v} \right)_{\hat{\Omega}}, \\ (u, \text{grad}\, \varphi)_{\Omega_q} &= \left(\det(DF_q)\, DF_q^{-T}\, \hat{u}, DF_q^{-T}\, \text{grad}\, \hat{\varphi} \right)_{\hat{\Omega}}, \\ (u, v)_{\Omega_q} &= \left(\det(DF_q)\, DF_q^{-T}\, \hat{u}, DF_q^{-T}\, \hat{v} \right)_{\hat{\Omega}}. \end{aligned}$$

In $d = 2$, the mapping of the curl-equation is given by

$$(\text{curl}\, u, \text{curl}\, v)_{\Omega_q} = \left(\frac{1}{\det(DF_q)}\, \text{curl}\, \hat{u}, \text{curl}\, \hat{v} \right)_{\hat{\Omega}}.$$

4 Eigenvalue Derivatives with Adjoint Calculus

For the calculation of the eigenvalue derivatives, we utilize the method of adjoint calculus inspired by a work of Heuveline and Rannacher [7] and Rannacher, Westenberger and Wollner [10], where this approach is applied to a posteriori error estimation for elliptic eigenvalue problems.

In the following, we assume the particular eigenvalue λ to be simple. Further, we assume that $u = u(q)$ and $\psi = \psi(q)$, because of the dependency of the control q to the mapping. For the calculation of eigenvalue derivative, we formulate the Lagrangian of the eigenvalue optimization problem

$$\begin{aligned} &\min_{(\lambda,q)}\ J(q,(\lambda,u)) \\ (\text{curl}\, u, \text{curl}\, v)_{\Omega_q} + (\text{grad}\, \psi, v)_{\Omega_q} &= \lambda(u,v)_{\Omega_q} \quad && \forall\, v \in H_0(\text{curl};\Omega_q) \\ (u, \text{grad}\, \varphi)_{\Omega_q} &= 0 && \forall\, \varphi \in H_0^1(\Omega_q) \\ \chi\left((u,u)_{\Omega_q} - 1\right) &= 0 && \forall\, \chi \in \mathbb{R}. \end{aligned} \tag{3}$$

The state variables are

$$(\lambda, (u, \psi)) \in \mathbb{R} \times (H_0(\text{curl};\Omega;\mathbb{R}^d) \times H_0^1(\Omega, \mathbb{R}^d)).$$

We define the corresponding adjoint variables with

$$(\mu, (z, \phi)) \in \mathbb{R} \times (H_0(\text{curl};\Omega;\mathbb{R}^d) \times H_0^1(\Omega, \mathbb{R}^d)).$$

Further, we simplify problem (3) by defining the equations

$$\begin{aligned} k(q,(u,\psi))(z,\phi) &= (\text{curl}\, u, \text{curl}\, z)_{\Omega_q} + (\text{grad}\, \psi, z)_{\Omega_q} + (u, \text{grad}\, \phi)_{\Omega_q}, \\ m(q,(u,\psi))(z,\phi) &= (u,z)_{\Omega_q}. \end{aligned}$$

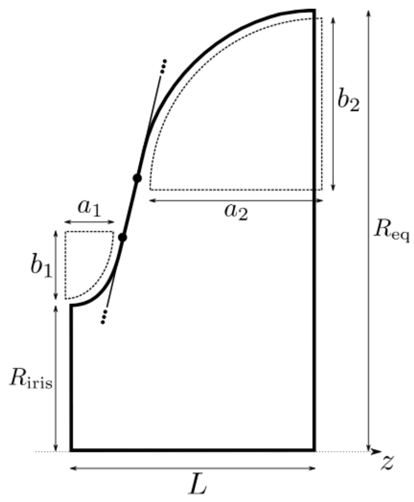

Fig. 2: Geometry of 1-cell TESLA cavity.

Table 1: Geometry data for the reference and deformed cavity

	reference cavity [B. Aune et al., 2000]	deformed cavity
	geometry (mm)	
R_{eq}	43.44542	45.00
R_{iris}	16.5627	16.5627
a_1	3.2	3.2
b_1	3.0592	3.0592
a_2	23.82353	23.82353
b_2	23.82352	23.82352
L	25.18	25.18

Table 2: Numerical solution of the first eigenvalues for the reference and deformed cavity

	reference cavity	deformed cavity
λ_0	1801.85	1679.74

With that, we define the Lagrangian for the admissible set Q^{ad}

$$\mathcal{L} : Q^{ad} \times (\mathbb{R} \times (H_0(\mathrm{curl};\Omega;\mathbb{R}^d) \times H_0^1(\Omega,\mathbb{R}^d))) \times (\mathbb{R} \times (H_0(\mathrm{curl};\Omega;\mathbb{R}^d) \times H_0^1(\Omega,\mathbb{R}^d)))$$

of problem (3) by

$$\begin{aligned}\mathcal{L}(q,(\lambda,(u,\psi)),(\mu,(z,\phi))) = J(q,(\lambda,u)) - k(q,(u,\psi))(z,\phi) + \lambda\, m(q,(u,\psi))(z,\phi) \\ + \mu\,(m(q,(u,\psi))(u,\psi) - 1)\,.\end{aligned}$$

By that, we define an optimality system of (3) which has the following form

$$\begin{aligned}\mathcal{L}'_{(\lambda,(u,\psi))}(q,(\lambda,(u,\psi)),(\mu,(z,\phi)))(\chi,(v,\varphi)) &= 0 \qquad \forall\,\chi,(v,\varphi) \in \mathbb{R} \times (H_0(\mathrm{curl};\Omega;\mathbb{R}^d) \times H_0^1(\Omega,\mathbb{R}^d)),\\ \mathcal{L}'_q(q,(\lambda,(u,\psi)),(\mu,(z,\phi)))\delta q &= 0 \qquad \forall\,\delta q \in Q^{ad},\\ \mathcal{L}'_{(\mu,(z,\phi))}(q,(\lambda,(u,\psi)),(\mu,(z,\phi)))(\chi,(v,\varphi)) &= 0 \qquad \forall\,\chi,(v,\varphi) \in \mathbb{R} \times (H_0(\mathrm{curl};\Omega;\mathbb{R}^d) \times H_0^1(\Omega,\mathbb{R}^d)).\end{aligned}$$

5 Discretization

For the discretization of the function spaces we apply the finite element method. We distinguish between the discretization of the function spaces $H_0^1(\Omega)$ and $H_0(\mathrm{curl};\Omega)$. We achieve the subspace $P_h \subset H_0^1(\Omega)$ by using node-based Lagrange elements. A discrete subspace $V_h \subset H_0(\mathrm{curl};\Omega)$, which ensures tangential continuity on the edges, is given by a discretization with edge-based Nédélec elements. For more details to finite elements and their properties, we refer to, e.g., Monk [9] and Boffi [3].

6 Numerical Examples

In this section, we present two numerical examples of the eigenvalue optimization of Maxwell's eigenvalue problem. For the optimization, we use the C++ library DOpElib [6] which is based on the finite element library deal.II [1]. For both examples, we consider the domain of a two-dimensional planar model, inspired by a 1-cell TESLA cavity, where the geometry is shown in Figure 2.

The Figure shows a quarter of the axis symmetrical model which is described by two radii, R_{eq} and R_{iris}, which are called radius of the equator and radius of the iris, as well as a length L and by two ellipses, defined by their axes. The ellipse next to the radius of the iris is defined by a horizontal half axis a_1 and a vertical half axis b_1, and the ellipse next to the equator is defined by a horizontal half axis a_2 and a vertical half axis b_2. The outer boundaries of the complete two-dimensional geometry are along the radius of the irises and along the boundaries of the ellipses.

For the reference geometry, we use the cavity data given in [2] and shown in Table 1 in the first column. For the discretization of the function spaces we are using the finite element discretization as mentioned before. To be more precise, we solve the optimization problem with Lagrange elements of order 1 and lowest order Nédélec elements. For the control the number of degree of freedom is 1122 and for the state the number of degree of freedom is 1633. The optimization problem is solved with a gradient descent algorithm which is implemented in the DOpElib library [6].

Table 3: Results of the last 5 iterations of example 1.

it	J	rel. Res.	λ_0
28	1.43594e+01	1.09840e-03	1801.80
29	1.43580e+01	8.64373e-04	1801.77
30	1.43575e+01	7.04101e-04	1801.75
31	1.43574e+01	6.02989e-04	1801.73
32	1.43574e+01	5.46530e-04	1801.73

Table 4: Results of the last 5 iterations of example 2.

it	J	rel. Res.	λ_0
35	3.12750e-04	2.40884e-04	1801.82
36	1.95372e-04	1.90140e-04	1801.83
37	1.22239e-04	1.50085e-04	1801.83
38	7.66714e-05	1.18469e-04	1801.83
39	7.66714e-05	9.35124e-05	1801.84

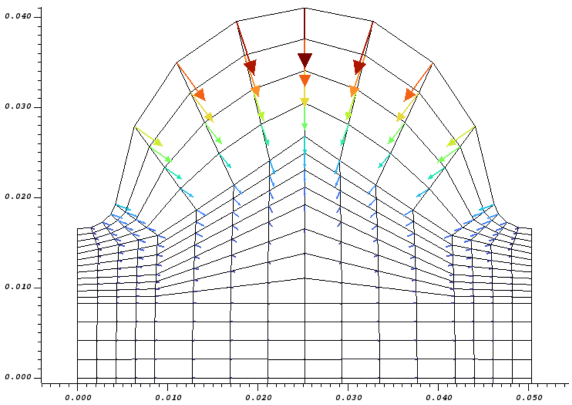

Fig. 3: Example 1: fixed iris. Deformation with scaling factor 5.

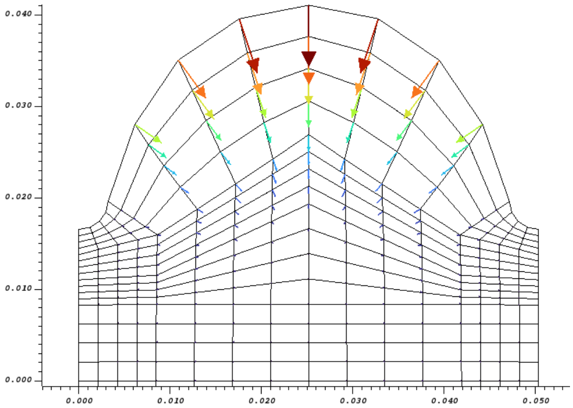

Fig. 4: Example 2: fixed iris and axes at iris. Deformation with scaling factor 5.

In these examples, we consider the optimization of the first (smallest) eigenvalue λ_0. We optimize on the known reference cavity, where the geometry parameters are mentioned in the first column of Table 1 and the numerically obtained first eigenvalue is $\lambda_0 = 1801.85$ (shown in the first column of Table 2). In the next step, we deform the cavity by increasing the radius of the equator (R_{eq}) from 43.44542mm to 45.00mm, see in the second column of Table 1. The corresponding numerically obtained value of the first eigenvalue is now $\lambda_0 = 1679.74$, see also the second column of Table 2.

The goal of this free-form optimization is to re-deform the deformed cavity to the reference geometry. Therefore, we consider two different examples:

In the first example, we fix the boundary on the irises (the part which is labeled with R_{iris} in Figure 2). The reduced gradient algorithm terminates after 32 iterations with the cost functional $J = 14.3574$ and a relative residual of $5.46530 \cdot 10^{-4}$. Furthermore, the eigenvalue λ_0 converges to $\lambda_0 = 1801.73$. The cost functionals J, relative residua and the first eigenvalue λ_0 after each iteration are shown in Table 3. The resulting deformation of the cavity with a scaling factor of 5 is shown in Figure 3. Although with fixing the boundary at the irises, the algorithm converges to the reference eigenvalue $\lambda_* = 1801.85$ but the original shape of the cavity cannot be exactly reconstructed. In this setting, the radius of the equator decreases and the shape of the ellipses at the equator as well as the ones at the irises deform, see Figure 3.

In the second example, we fix again the boundary on the irises and, in addition, we fix the boundary curve given by the first ellipse (a_1, b_1) to ensure no deformation at those. The reduced gradient algorithm terminates after 39 iterations with the cost functional $J = 7.66714 \cdot 10^{-5}$ and the relative residual of $9.35124 \cdot 10^{-5}$. Furthermore, the eigenvalue λ_0 converges to $\lambda_0 = 1801.84$. In this setting, we ensure that the deformation of the geometry has just influence in the radius of the equator (R_{eq}) which was desired. The resulting deformation of the cavity with a scaling factor of 5 is shown in Figure 4. The cost functionals J, relative residua and the first eigenvalue λ_0 after each iteration are shown in Table 4.

7 Conclusion and Outlook

We have derived an optimization problem for Maxwell's eigenvalue problem for simple eigenvalues inspired by particle accelerator cavity design. In the cost functional, we considered the optimization of one particular eigenvalue. For the numerical approach, we introduced a mixed finite element method by means of Nédélec and Lagrange elements and for the optimization itself, we introduced the first eigenvalue derivatives derived with adjoint calculus. In the numerical examples, we showed the convergence of the optimization problem for two examples on a two-dimensional cavity domain.

There are still some open tasks. Because we are interested in a real-world simulation of these cavities, it is quite obvious that we need a more realistic model of the considered problem. First, an extension to a multi-cell cavity is natural, mentioned in [5]. Thereby, a cost functional with respect to the corresponding eigenvector of the particular eigenvalue will be relevant to also optimize the flatness of the model. So far the two-dimensional examples are also only considered in plane. An area of interest is the extension of the formulation of a three-dimensional Maxwell's eigenvalue problem which is either possibly by extending the domain itself to 3D or by taking the advantage of rotation symmetry of the two-dimensional geometry.

Acknowledgements Open access funding enabled and organized by Projekt DEAL.

References

[1] D. Arndt, W. Bangerth, B. Blais, T. C. Clevenger, M. Fehling, A. V. Grayver, T. Heister, L. Heltai, M. Kronbichler, M. Maier, P. Munch, J.-P. Pelteret, R. Rastak, I. Thomas, B. Turcksin, Z. Wang, and D. Wells, *The `deal.II` library, version 9.2*, Journal of Numerical Mathematics, 28 (2020), pp. 131–146.

[2] B. Aune, R. Bandelmann, D. Bloess, B. Bonin, A. Bosotti, M. Champion, C. Crawford, G. Deppe, B. Dwersteg, D. A. Edwards, H. T. Edwards, M. Ferrario, M. Fouaidy, P.-D. Gall, A. Gamp, A. Gössel, J. Graber, D. Hubert, M. Hüning, M. Juillard, T. Junquera, H. Kaiser, G. Kreps, M. Kuchnir, R. Lange, M. Leenen, M. Liepe, L. Lilje, A. Matheisen, W.-D. Möller, A. Mosnier, H. Padamsee, C. Pagani, M. Pekeler, H.-B. Peters, O. Peters, D. Proch, K. Rehlich, D. Reschke, H. Safa, T. Schilcher, P. Schmüser, J. Sekutowicz, S. Simrock, W. Singer, M. Tigner, D. Trines, K. Twarowski, G. Weichert, J. Weisend, J. Wojtkiewicz, S. Wolff, and K. Zapfe, *Superconducting tesla cavities*, Phys. Rev. ST Accel. Beams, 3 (2000), p. 092001.

[3] D. Boffi, *Finite element approximation of eigenvalue problems*, Acta Numer., 19 (2010), pp. 1–120.

[4] G. Cohen, *Higher-Order Numerical Methods for Transient Wave Equations*, Scientific computation, Springer, 2002.

[5] J. Corno, *Numerical Methods for the Estimation of the Impact of Geometric Uncertainties on the Performance of Electromagnetic Devices*, PhD thesis, Technische Universität, Darmstadt, 2017.

[6] C. Goll, T. Wick, and W. Wollner, *DOpElib: Differential equations and optimization environment; A goal oriented software library for solving pdes and optimization problems with pdes*, Archive of Numerical Software, 5 (2017), pp. 1–14.

[7] V. Heuveline and R. Rannacher, *A posteriori error control for finite approximations of elliptic eigenvalue problems*, Adv. Comput. Math., 15 (2001), pp. 107–138.

[8] F. Kikuchi, *Mixed and penalty formulations for finite element analysis of an eigenvalue problem in electromagnetism*, Applied Mechanics and Engineering, 64 (1987), pp. 509–521.

[9] P. Monk, *Finite Element Methods for Maxwell's Equations*, Oxford University Press, 04 2003.

[10] R. Rannacher, A. Westenberger, and W. Wollner, *Adaptive finite element solution of eigenvalue problems: Balancing of discretization and iteration error*, Journal of Numerical Mathematics, 18 (2010), pp. 303–327.

